Molecular Saddles. 7.[1] New 9,10-Bis(1,3-dithiol-2-ylidene)-9,10-dihydroanthracene Cyclophanes: Synthesis, Redox Properties, and X-ray Crystal Structures of Neutral Species and a Dication Salt

Christian A. Christensen, Andrei S. Batsanov, Martin R. Bryce,* and Judith A. K. Howard

Department of Chemistry, University of Durham, Durham DH1 3LE, UK

m.r.bryce@durham.ac.uk

Received October 26, 2000 (Revised Manuscript Received February 16, 2001)

We report the synthesis of cyclophanes **18**−**20** by ester-forming macrocyclization reactions of diols **15** and **16** with 1,4-benzenedicarbonyl chloride. Compounds **18** and **19** display a two-electron, quasireversible oxidation wave in the cyclic voltammogram to yield the dication species at E^{ox}_{pa} 0.52 and 0.47 V, respectively (vs Ag/AgCl in acetonitrile), whereas the 2 + 2 product **20** undergoes a single four-electron oxidation process at E^{ox}_{pa} 0.51 V. X-ray crystal structures are reported for compounds **18**−**20** and the dication salt $\mathbf{18}^{2+}(I_3^-)_2{\cdot}(I_2)_{0.5}$. For comparative purposes, the structures are also reported for the precursor diol **15** and its dication salt $\mathbf{15}^{2+}(ClO_4^-)_2$, which was obtained by electrocrystallization. In the neutral cyclophanes **18**−**20**, the 9,10-bis(1,3-dithiol-2-ylidene)-9,10-dihydroanthracene moieties adopt a saddle-shaped conformation. The overall measure of folding, the dihedral angle (θ) between the S(1)C(16)C(17)S(2) and S(5)C(21)C(22)S(6) planes, is similar in **15** and **18** (87.6° and 83.7°, respectively) whereas this angle is significantly narrower in **19** (61.1°), illustrating the flexibility of the saddle conformation and its dependence on the packing. Dimeric molecule **20** contains two saddle moieties with very similar conformations, θ = 73.4° and 73.1°. The structures of dication salts $\mathbf{15}^{2+}(ClO_4^-)_2$ and $\mathbf{18}^{2+}(I_3^-)_2{\cdot}(I_2)_{0.5}$ reveal that a dramatic conformational change accompanies oxidation of the donor with the dithiolium rings planar and nearly perpendicular to the mean plane of the anthracene moieties. A notable feature of $\mathbf{18}^{2+}$ is that the bridge enforces a fold of 22° along the C(9)...C(10) vector of the anthracene unit. In $\mathbf{15}^{2+}$ there is no fold about this axis, instead the anthracene moiety is slightly twisted with the two (planar) outer rings forming an angle of 7°.

Introduction

It is known that the central *p*-quinodimethane ring of 9,10-bis(1,3-dithiol-2-ylidene)-9,10-dihydroanthracene adopts a boat conformation due to steric interactions between the *peri*-hydrogens and the sulfur atoms, and thereby the molecule adopts a saddle shape.[2] The bis-(1,3-dithiole) substituents impart strong π-electron donor properties to the system,[3] e.g., compound **1**[2b] (Chart 1) undergoes a single, two-electron, quasireversible redox wave to yield a thermodynamically stable dication at E^{ox} ca. +0.45 V (vs Ag/AgCl in MeCN) in the cyclic voltammogram (CV). At this redox stage there is gain of aromaticity in the central anthracene unit and in the 6 π-electron dithiolium cations. A major conformational change accompanies the oxidation process: X-ray crystallography has established that 9,10-bis(1,3-dithiol-2-ylidene)-9,10-dihydroanthracene dications have a planar anthracene system with the 1,3-dithiolium cations almost orthogonal to this plane.[2a,4] Theoretical calculations support the electrochemical and crystallographic data.[5]

Chart 1

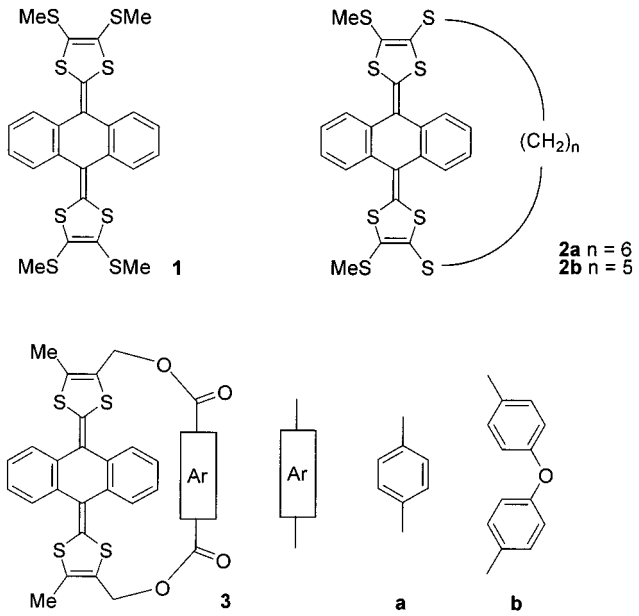

(1) Part 6: Jones, A. E.; Christensen, C. A.; Perepichka, D. F.; Batsanov, A. S.; Beeby, A.; Low, P. J.; Bryce, M. R.; Parker, A. W. *Chem. Eur. J.* **2001**, *7*, 973.

(2) (a) Bryce, M. R.; Moore, A. J.; Hasan, M.; Ashwell, G. J.; Fraser, A. T.; Clegg, W.; Hursthouse, M. B.; Karaulov, A. I. *Angew. Chem., Int. Ed. Engl.* **1990**, *29*, 1450. (b) Batsanov, A. S.; Bryce, M. R.; Coffin, M. A.; Green, A.; Hester, R. E.; Howard, J. A. K.; Lednev, I. K.; Martín, N.; Moore, A. J.; Moore, J. N.; Ortí, E.; Sánchez, L.; Savíron, M.; Viruela, P. M.; Viruela, R.; Ye, T.-Q. *Chem. Eur. J.* **1998**, *4*, 2580. (c) Bryce, M. R.; Finn, T.; Moore, A. J.; Batsanov, A. S.; Howard, J. A. K. *Eur. J. Org. Chem.* **2000**, 51.

(3) (a) Bryce, M. R.; Coffin, M. A.; Hursthouse, M. B.; Karaulov, A. I.; Müllen, K.; Scheich, H. *Tetrahedron Lett.* **1991**, *32*, 6029. (b) Moore, A. J.; Bryce, M. R. *J. Chem. Soc., Perkin Trans. 1* **1991**, 157. (c) Liu, S.-G.; Pérez, I.; Martín, N.; Echegoyen, L. *J. Org. Chem.* **2000**, *65*, 9092.

10.1021/jo001524k CCC: $20.00 © 2001 American Chemical Society
Published on Web 04/14/2001

Derivatives of this extended π-donor system are currently being studied as components of inter-[4b,6] and intramolecular[7] charge-transfer systems.

Cyclophanes are well-known building blocks in the fields of macrocyclic and supramolecular chemistry[8] with redox-active systems,[9,10] notably tetrathiafulvalene derivatives,[9] attracting current attention. We have recently synthesized the first cyclophane structures **2** and **3** (Chart 1) which incorporate the 9,10-bis(1,3-dithiol-2-ylidene)-9,10-dihydroanthracene framework.[11] The oxidation potentials of **2a**,[11a] **2b**,[11a] and **3a**[11b] were raised significantly to E^{ox}_{pa} = ca. 0.70 V compared with those of nonbridged analogues, whereas for **3b** E^{ox}_{pa} = 0.47 V (vs Ag/AgCl in MeCN). The raised oxidation potentials for **2a**, **2b**, and **3a** reflect the reduced stability of the twisted dication structure within the steric constraints of the smaller cyclophanes.

Results and Discussion

We now describe new 9,10-bis(1,3-dithiol-2-ylidene)-9,10-dihydroanthracene cyclophanes **18**−**20** which are formed by bridging across the 2,6-positions of the anthracene unit, as opposed to bridging across the dithiole rings, as was the case in the previous examples **2** and **3**.[11] This new position of bridging has the attraction that, unlike **2** and **3**, mixtures of geometric isomers cannot be formed in the cyclization reactions. The aim of this work is to probe further the effects of steric constraints on the redox and structural properties of the system in both the neutral and dication forms. The synthetic methodology involves ester-forming macrocyclization reactions of the precursor diol derivatives **15** and **16**. Redox properties and X-ray crystal structures of the cyclophanes are reported, along with structures of the dication salts $\mathbf{15}^{2+}(ClO_4^-)_2$ and $\mathbf{18}^{2+}(I_3^-)_2{\cdot}(I_2)_{0.5}$.

Synthesis. We identified 2,6-dihydroxyanthraquinone **9** as an appropriate readily available starting material for the synthesis of our target cyclophanes. For attachment of oxyethylene chains to the hydroxy groups of **9**, we prepared reagents **6** and **8** in high yields using standard procedures as shown in Scheme 1. Reactions of **9** with **6** and **8**, in the presence of potassium carbonate, cleanly afforded compounds **10** and **11**, which then underwent 2-fold Horner−Wadsworth−Emmons olefination upon reaction with the anion generated by treatment of phosphonate ester reagent **12**[12] with lithium diisopropylamide (LDA) at −78 °C, to yield the 9,10-bis(1,3-dithiol-2-ylidene)-9,10-dihydroanthracene derivatives **13** and **14** in 69 and 81% yields, respectively (Scheme 2). Removal of the silyl protecting groups with tetrabutylammonium fluoride readily afforded diol derivatives **15**

Scheme 1

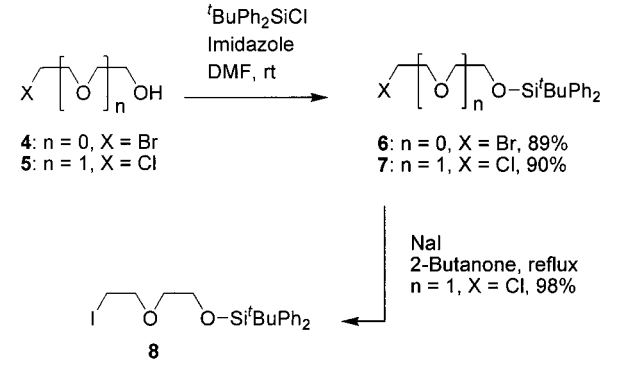

Scheme 2

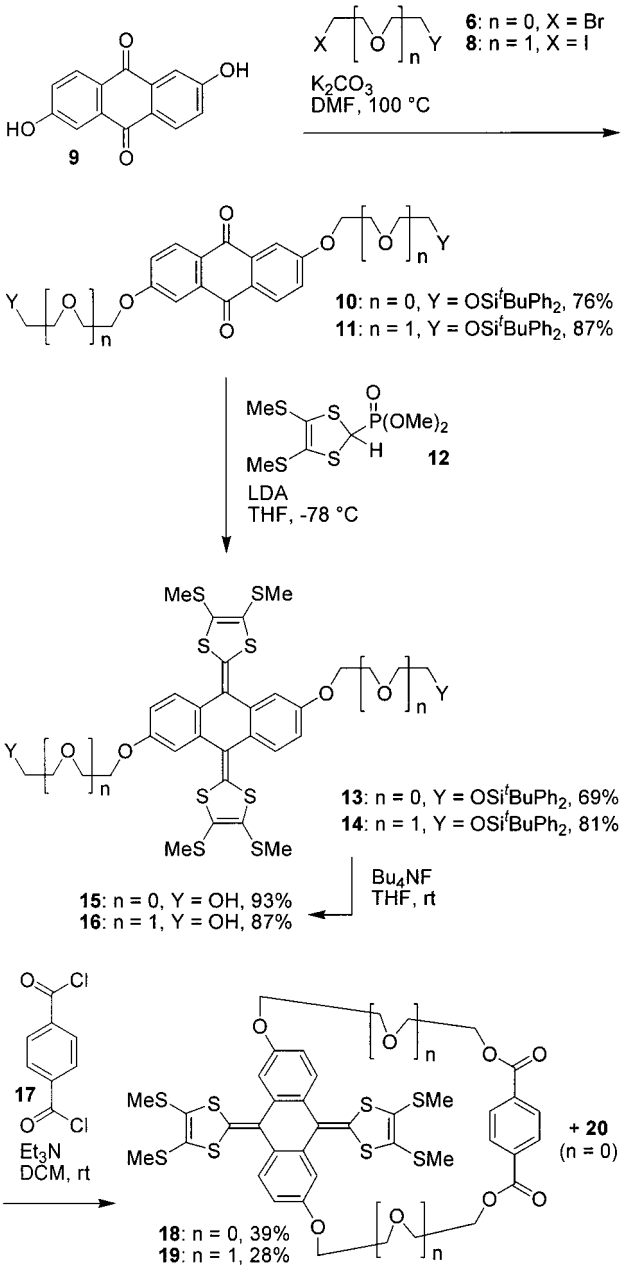

(4) (a) Triki, S. Ouahab, L.; Lorcy, D.; Robert, A. *Acta Crystallogr.* **1993**, *C49*, 1189. (b) Bryce, M. R.; Finn, T.; Batsanov, A. S.; Kataky, R.; Howard, J. A. K.; Lyubchik, S. B. *Eur. J. Org. Chem.* **2000**, 1199.

(5) Martín, N.; Sánchez, L.; Seoane, C.; Ortí, E.; Viruela, P. M.; Viruela, R. *J. Org. Chem.* **1998**, *63*, 1268.

(6) Gautier, N.; Mercier, N.; Riou, A.; Gorgues, A.; Hudhomme, P. *Tetrahedron Lett.* **1999**, *40*, 5997.

(7) (a) Herranz, M. A.; Martín, N. *Org. Lett.* **1999**, *1*, 2005. (b) Christensen, C. A.; Bryce, M. R.; Batsanov, A. S.; Howard, J. A. K.; Jeppersen, J. O.; Becher, J. *Chem. Commun.* **2000**, 113.

(8) Vögtle, F. *Cyclophane Chemistry*; Wiley: Chichester, 1993.

(9) (a) Otsubo, T.; Aso, Y.; Takimiya, K. *Adv. Mater.* **1996**, *8*, 203. (b) Batsanov, A. S.; John, D. E.; Bryce, M. R.; Howard, J. A. K. *Adv. Mater.* **1998**, *10*, 1360. (c) Akutagawa, T.; Abe, Y.; Hasegawa, T.; Nakamura, T.; Inabe, T.; Sugiura, K.; Sakata, Y.; Christensen, C. A.; Lau, J.; Becher, J. *J. Mater. Chem.* **1999**, *9*, 2737. (d) Nielsen, M. B.; Lomholt, C.; Becher, J. *Chem. Soc. Rev.* **2000**, *29*, 153. (e) Bryce, M. R. *J. Mater. Chem.* **2000**, *10*, 589.

(10) Hascot, P.; Lorcy, D.; Robert, A.; Boubekeur, K.; Batail, P, Carlier, R.; Tallec, A. *J. Chem. Soc., Chem. Commun.* **1995**, 1229.

(11) (a) Finn, T.; Bryce, M. R.; Batsanov, A. S.; Howard, J. A. K. *Chem. Commun.* **1999**, 1835. (b) Godbert, N.; Batsanov, A. S.; Bryce, M. R.; Howard, J. A. K. *J. Org. Chem.* **2001**, *66*, 713.

(12) Moore, A. J.; Bryce, M. R. *Tetrahedron Lett.* **1992**, *33*, 1373.

Chart 2

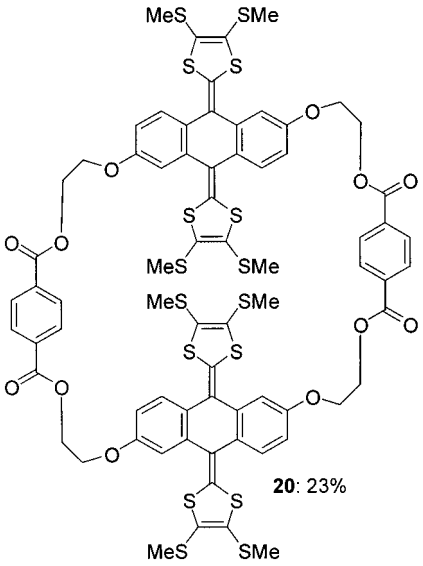

and **16** in high yields. Cyclization reactions with 1,4-benzenedicarbonyl chloride in the presence of triethylamine gave the cyclophane derivatives **18** and **19**, in 39 and 28% yields, respectively. The 2 + 2 cyclophane **20** (Chart 2) was also isolated in 23% yield. Compounds **18**−**20** are air-stable yellow solids.

The ^{1}H NMR spectrum shows that the 2 + 2 cyclophane **20** is present as two conformers, clearly seen from the two singlets (each integrating to four protons) arising from the phenyl protons at 7.98 and 7.94 ppm, respectively. Also the doublets, and the doublet of doublets, characteristic of 2,6-substituted anthraquinone derivatives, are seen as pairs, indicative of the two conformers. Another interesting feature of the ^{1}H NMR's for the cyclophanes is the chemical shift of the singlet arising from the phenyl protons. For **18**, the short-bridged cyclophane, the singlet is observed at 6.89 ppm, whereas for **19** it is at 7.35 ppm. Hence the chemical shift of the phenyl protons is indicative of the length of the bridge, and consequently how close the phenyl ring is positioned to the anthracene ring system, with a change of 1 ppm from the short-bridged **18** to the longest bridged 2 + 2 cyclophane **20**, in which the phenyl rings can be far removed from the anthracene ring system.

The dication salt $\mathbf{15}^{2+}(ClO_4^-)_2$ was obtained by electrocrystallization of **15** using tetrabutylammonium perchlorate as the electrolyte in dichloromethane. Salt $\mathbf{18}^{2+}(I_3^-)_2{\cdot}(I_2)_{0.5}$ was obtained by diffusion of iodine vapor into a solution of **18** in dichloromethane.

Solution Electrochemistry. Solution electrochemical data, obtained by cyclic voltammetry (CV), are collated in Table 1. All the nonbridged systems **13**−**16** showed the quasireversible two-electron redox wave (neutral → dication species) typical for 9,10-bis(1,3-dithiol-2-ylidene)-9,10-dihydroanthracene derivatives,[3] but with a positive shift compared to the unsubstituted system due to the four electron-withdrawing alkylsulfanyl substituents, a trend well-known from derivatives of tetrathiafulvalene (TTF).[13] Comparison of cyclophanes **18** and **19** with the precursors **15** and **16** reveals some interesting trends. The oxidation potential (E^{ox}_{pa}) is raised by 50 mV for **18**, but no increase is seen for **19**. This is consistent with the shorter bridge of **18** obstructing the marked conformational change which accompanies oxidation to the dication (see the crystal structure of $\mathbf{18}^{2+}$) whereas the longer bridge of **19** allows free conformational change. These observations are in good agreement with the oxidation potentials of **3a** and **3b** studied previously.[11b] A rise of 300 mV was observed for the short-bridged system **3a**, whereas only a slight rise was seen for **3b** incorporating the longer bridge. The increase in oxidation potential is obviously more significant when the two dithiole rings are bridged, since upon oxidation they undergo a more dramatic conformational change than the anthracene ring system. Consistent with this, ΔE (defined as $E^{ox}_{pa} - E^{ox}_{pc}$) is significantly reduced for compound **3a** (i.e., increased reversibility of the oxidation process) due to the short bridge preventing a big conformational change, whereas no significant difference in ΔE is observed for **18** or **19** compared to that of their precursors. The 2 + 2 cyclophane **20** showed one, slightly broadened, quasireversible redox wave, presumably a four-electron process forming the $\mathbf{20}^{4+}$ species. The oxidation potential was raised by 40 mV compared to that of its precursor **15**, which we ascribe to a combination of intramolecular Coulombic repulsion between the two dication units and the steric constraints in the oxidized cyclophane system.

Table 1. Cyclic Voltammetric Data[a]

compd	E^{ox}_{pa}/V	E^{ox}_{pc}/V	ΔE/V[b]
13	0.47 (2e)	0.34	0.13
14	0.46 (2e)	0.37	0.09
15	0.47 (2e)	0.29	0.18
16	0.46 (2e)	0.36	0.10
18	0.52 (2e)	0.41	0.11
19	0.47 (2e)	0.33	0.14
20	0.51 (4e)	0.37	0.14

[a] Compound ca. 2×10^{-3} M, vs Ag/AgCl, electrolyte $Bu_4N^+PF_6^-$, acetonitrile, 20 °C, scan rate 100 mV s^{-1}. Data obtained on a BAS CV50W voltammetric analyzer with *iR* compensation. [b] $\Delta E = E^{ox}_{pa} - E^{ox}_{pc}$ (E^{ox}_{pa} is the oxidation peak potential on the first anodic scan; E^{ox}_{pc} is the coupled reduction peak potential on the cathodic scan).

Table 2. Dihedral Angles (deg) in Neutral Molecules

	15		**18**	**19**	**20**	
φ	36.4	39.2	35.7	37.1	34.6	37.3
δ_1	8.4	17.9	19.3	16.6	15.6	19.4
δ_2	2.8	19.4	0	22.1	13.7	11.3
θ	79.1	87.6	83.7	61.1	73.4	73.1

X-ray Crystal Structures. The cyclophanes **18** and **19** and the nonbridged precursor **15** have saddlelike conformations similar to those described earlier for nonbridged analogues[2] and those with a bridge between the dithiole rings.[11] Molecular structures are shown in Figure 1, and principal conformational parameters are given in Table 2. Crystals of **18** and **19** contain no solvent of crystallization. Folding (φ) of the anthraquinone moiety along the C(9)...C(10) vector is not affected significantly by the bridge. Both structures show the usual packing motif[2] of pseudodimers of molecules with mutually engulfing U-shaped bis(dithiole)anthraquinone moieties (Figure 2). However, the folding of these moieties is significantly different. The overall measure of the U-bend, the dihedral angle (θ) between the S(1)C(16)C(17)S(2) and S(5)C(21)C(22)S(6) planes in **18** (83.7°) is within the range (76−92°) observed in nonbridged systems,[2] including **15**. In **19** this angle (61.1°) is almost as

(13) Moore, A. J.; Bryce, M. R. *J. Chem. Soc., Chem. Commun.* **1991**, 1638.

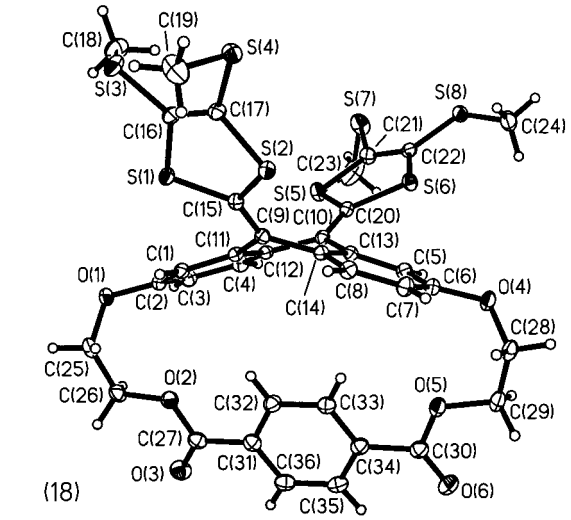

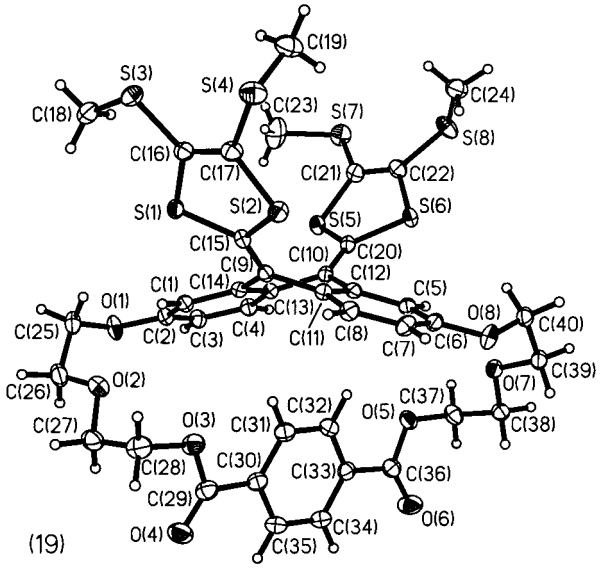

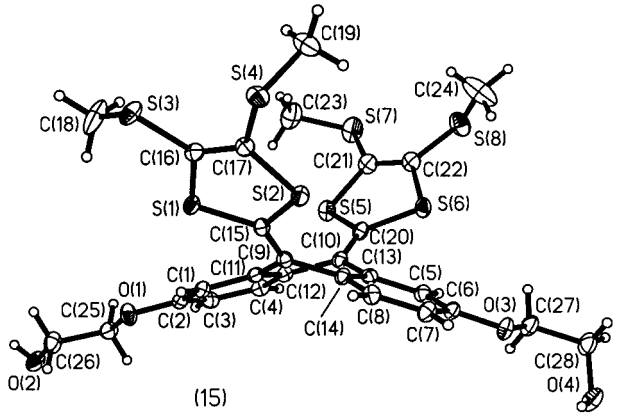

Figure 1. Molecular structures of **18**, **19**, and **15**, showing 50% thermal ellipsoids.

narrow as in **2a** and **2b** (46−54°). This illustrates the flexibility of the saddle conformation and its dependence on the packing.

Compound **15** crystallizes from dichloromethane/hexane solution as a mixed solvate. The asymmetric unit comprises two molecules of **15** (A and B), three CH_2Cl_2 molecules (two of them disordered) and half of a hexane molecule, which occupies a cavity around an inversion

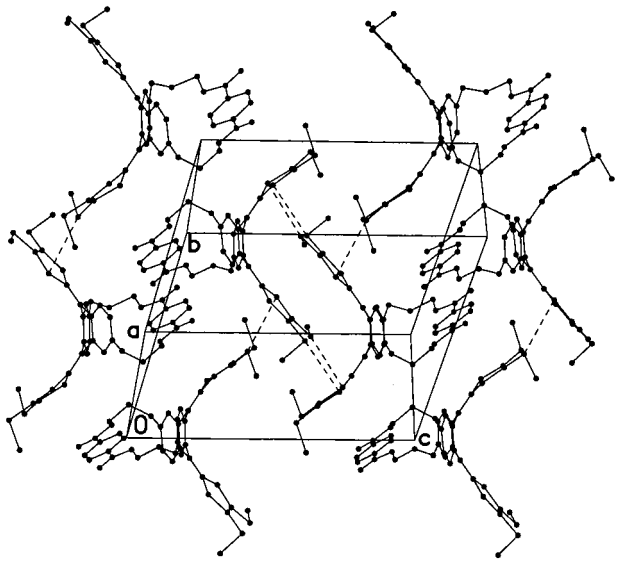

Figure 2. Crystal packing of **18**, showing short S...S contacts (3.55−3.64 Å).

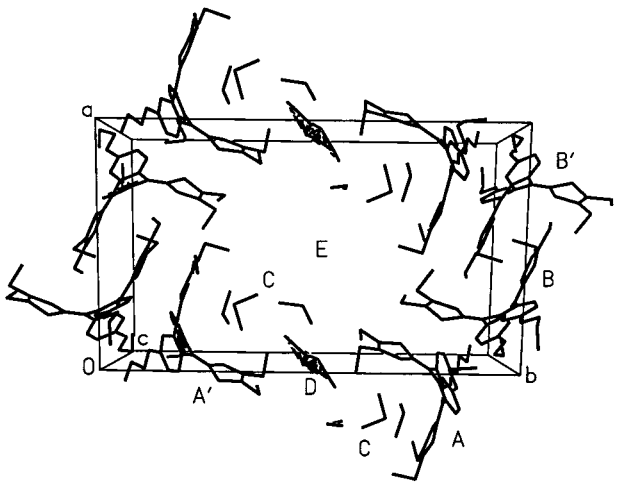

Figure 3. Crystal packing of **15**. Molecule A and its inversion equivalent A′ enclose solvent molecules of CH_2Cl_2 (C, disorder not shown) and hexane (D, disordered around an inversion center). Molecule B and its inversion equivalent B′ form a mutually engulfing dimer. The apparent gap E is filled by hydroxyethyleneoxo chains of type B molecules lying above and below the layer.

center and is chaotically disordered therein (Figure 3). All the OH groups participate in strong (O...O 2.63−2.79 Å, O−H−O 154−178°) hydrogen bonds with each other. Dimeric molecule **20** (Figure 4) contains two saddle units (in approximately parallel orientation) forming mutually engulfing interactions with two other molecules, related to the first via different inversion centers (Figure 5). Intramolecular self-engulfing does not occur. The conformations of the two saddle units are very similar; one of the SMe groups shows a disorder of the sulfur atom. The structure contains infinite channels, running along the *y* axis and filled with chaotically disordered solvent of crystallization, which we believe to be a mixture of CH_2Cl_2 and hexane, partially sharing the same sites. The volume of the channel and the electron density distribution are in agreement with a **20**:CH_2Cl_2:hexane stoichiometry of 1:1:1.

The asymmetric unit of the iodide salt of **18** comprises one $[\mathbf{18}]^{2+}$ dication, two triiodide anions, half of an I_2

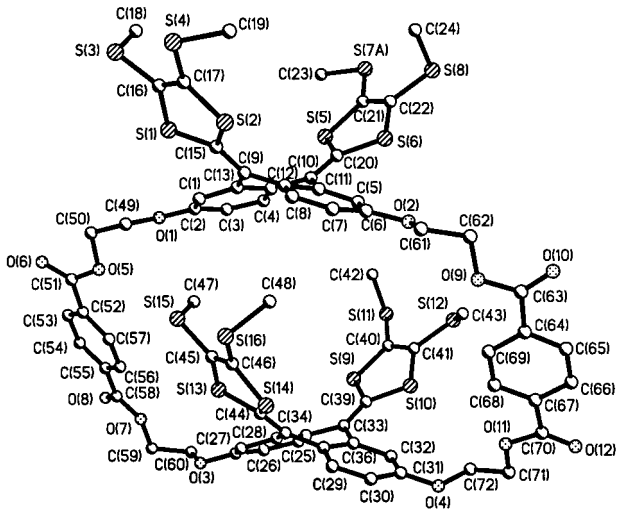

Figure 4. Molecular structure of **20**. The minor position of the disordered S(7) atom and all H atoms are omitted.

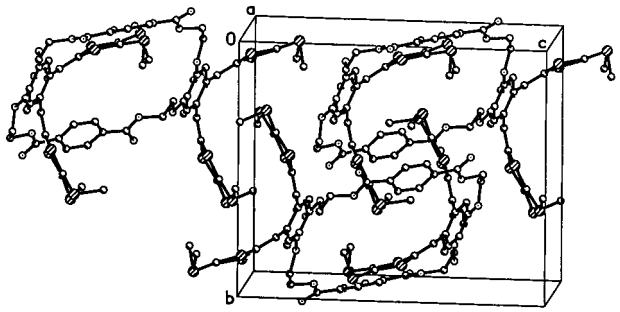

Figure 5. Crystal packing of **20**.

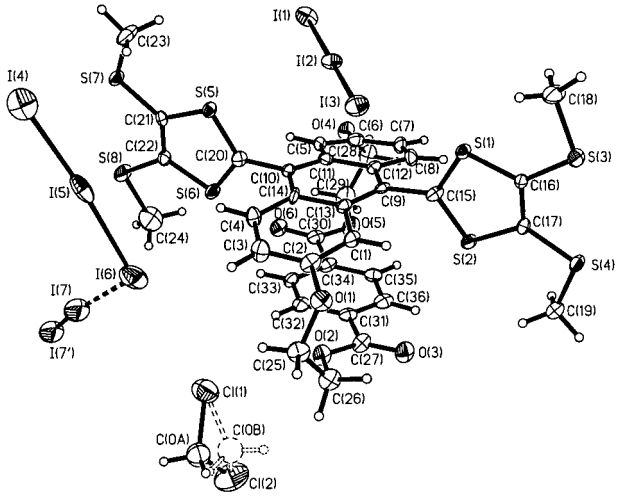

Figure 6. Asymmetric unit of $\mathbf{18}^{2+}(I_3^-)_2 \cdot (I_2)_{0.5} \cdot CH_2Cl_2$ [I(7′) is related to I(7) by an inversion center], showing 50% thermal ellipsoids. Angles in degrees: I(1)−I(2)−I(3) 176.94(3), I(4)−I(5)−I(6) 175.19(3), I(5)−I(6)−I(7) 107.66(4), I(6)−I(7)-I(7′) 168.29(6).

molecule (which is situated at an inversion center), and one disordered CH_2Cl_2 molecule (Figure 6). The iodine molecule has a I(7)−I(7′) bond distance of 2.766 Å and forms secondary bonds I(6)...I(7) 3.378(2) Å with two anions, causing considerable asymmetric bond distances therein: I(4)−I(5) 2.873(2) vs I(5)−I(6) 2.988(2) Å. The shortest I...I contact formed by the other independent anion, I(3)...I(7) of 4.30 Å, is equal to double the van der

Chart 3

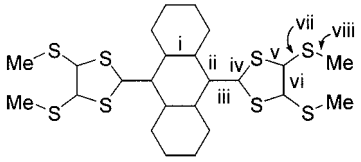

Waals radius. Correspondingly, the I(1)−I(2) and I(2)−I(3) bonds in it are practically equal, 2.930(1) and 2.918(1) Å. There is no continuous polyiodide motif.

Oxidation of **18** to $\mathbf{18}^{2+}$ results in a profound electronic and conformational rearrangement, as in nonbridged analogues.[2a,4] The anthracenediylidene moiety is converted into an aromatic anthracene system the planarity of which, however, is perturbed by the bridge. Two modes of distortion of an anthracene system have been observed earlier. In 9,10-bridged anthracenophanes[14a] the anthracene system is folded (by φ angle, see above) along the C(9)...C(10) vector, with the central anthracene ring adopting a boat conformation. The nonbridged, anthracene systems, which are overcrowded with substituents, adopt an "end-to-end twist", measured by the angle (τ) between the C(2)−C(3) and C(5)−C(6) bonds ($\tau = 0$ for the planar anthracene).[14b] In $\mathbf{3b}^{2+}$ the bridge between the dithiole ring effects a minor ($\varphi = 6°$) folding and practically no end-to-end twist of the anthracene system. In $\mathbf{18}^{2+}$ both the twist ($\tau = 7°$) and folding ($\varphi = 22°$) are substantial. Strictly speaking, C(9) and C(10) are not coplanar with the outer anthracene rings and therefore the distortion is not a simple folding. It can be described by the dihedral angles α between the central C(11)C(12)C(13)C(14) plane and the C(9)C(11)C(14) or C(10)C(12)C(13) planes, the tilting angle β between the latter two planes and the C(9)−C(15) and C(10)−C(20) bonds, respectively, and dihedral angles γ between the C(11)C(12)C(13)C(14) plane and the planes of the outer anthracene rings. The average $\alpha = 6.8°$, $\beta = 3.6°$, and $\gamma = 11.0°$ in $\mathbf{18}^{2+}$ are significantly smaller than those in tetramethyl[6]-9,10-anthracenophane ($\alpha = 24.7°$, $\beta = 18.5°$, and $\gamma = 10.4°$) and tetraphenyl[6]-9,10-anthracenophane ($\alpha = 23.0°$, $\beta = 19.8°$, and $\gamma = 2.4°$)[14a] in which the bond distances in the outer anthracene rings do not differ from those in anthracene itself,[14c] but the bonds between these rings and C(9) or C(10) are weaker (1.418−1.422 Å vs 1.399 Å in anthracene), due to the nonplanarity interfering with the p-orbital overlap. In the less distorted $\mathbf{18}^{2+}$, these bonds (ii, see Table 3 and Chart 3) average 1.41(1) Å. The bridging benzene ring is practically parallel and eclipsed with the central anthracene ring, resulting in intramolecular contacts C(13)...C(31) 3.58, C(10)...C(33) 3.60, and C(11)...C(34) 3.56 Å, while in neutral **18** and **19** this benzene ring is inclined to the C(11)C(12)C(13)C(14) plane by 60° and 79°, respectively.

The asymmetric unit of the salt $\mathbf{15}^{2+}(ClO_4^-)_2$ comprises one $\mathbf{15}^{2+}$ dication, two perchlorate anions, and one CH_2Cl_2 molecule (Figure 7). Intermolecular hydrogen bonds O(2)−H...O(4) and O(4)−H...O(1) (O...O 2.93 and 2.84 Å, O−H−O 149−161°) link cations (related by the *b* translation) into an infinite chain, parallel to the *y* axis. In

(14) (a) Tobe, Y.; Saiki, S.; Utsumi, N.; Kusumoto, T.; Ishii, H.; Kakiuchi, K.; Kobiro, K.; Naemura, K. *J. Am. Chem. Soc.* **1996**, *118*, 9488. (b) Pascal, R. A.; McMillan, W. D.; van Engen, D.; Eason, R. G. *J. Am. Chem. Soc.* **1987**, *109*, 4660. (c) Pratt Brock, C.; Dunitz, J. D. *Acta Crystallogr.* **1990**, *B46*, 795.

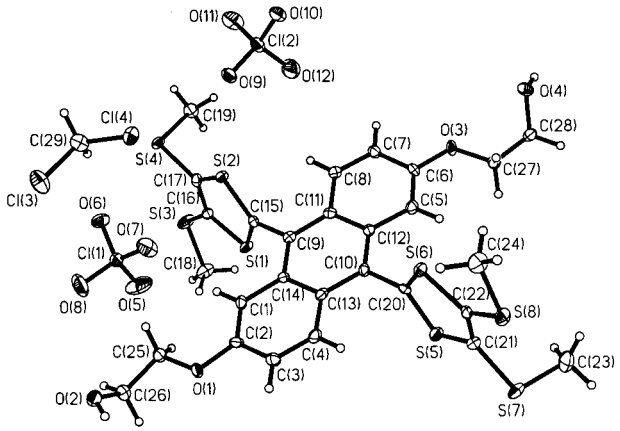

Figure 7. Asymmetric unit of $\mathbf{15}^{2+}(ClO_4^-)_2 \cdot CH_2Cl_2$, showing 50% thermal ellipsoids.

Table 3. Average Bond Distances

	15	$\mathbf{15}^{2+}$	**18**	$\mathbf{18}^{2+}$	**19**	**20**
i	1.417(4)	1.435(6)	1.420(2)	1.45(1)	1.412(2)	1.415(8)
ii	1.482(4)	1.405(6)	1.481(2)	1.41(1)	1.483(2)	1.462(8)
iii	1.361(4)	1.487(6)	1.364(2)	1.50(1)	1.359(2)	1.352(8)
iv	1.769(3)	1.686(5)	1.772(1)	1.678(8)	1.774(2)	1.762(6)
v	1.759(3)	1.719(5)	1.757(1)	1.717(7)	1.763(2)	1.752(7)
vi	1.343(4)	1.376(6)	1.347(2)	1.38(1)	1.346(2)	1.328(9)
vii	1.753(3)	1.733(5)[a] 1.760(5)[b]	1.753(1)	1.740(8)[a]	1.757(2)	1.749(8)
viii	1.805(4)	1.797(5)[a] 1.814(5)[b]	1.812(2)	1.799(9)[a]	1.811(2)	1.793(9)

[a] In-plane SMe group. [b] Out-of-plane SMe group.

contrast with $\mathbf{18}^{2+}$, the anthracene moiety in $\mathbf{15}^{2+}$ is not folded along the C(9)...C(10) vector, but the end-to-end twist ($\tau = 10.6°$) is even stronger than in the former, although the bridge is absent. Both dithiolium rings are planar and nearly coplanar (within 5°) and both are nearly perpendicular to the mean plane of the anthracene moiety, forming dihedral angles of 78° and 83° with it. The O(1)C(25)C(26) and O(3)C(27)C(28) side chains are essentially coplanar with the anthracene system, while the O(2)H and O(4)H hydroxy groups are oriented out of the plane on the same side of it. The asymmetric unit contains six cation−anion S...O contacts shorter than the standard van der Waals distance of 3.25 Å, the shortest being S(6)...O(8) 3.01 Å and S(2)...O(9) 3.08 Å.

As would be expected, the C−S bonds in the dithiole rings are shortened, and the C=C bond lengthened on oxidation, as the ring acquires more aromatic character (Table 3 and Chart 3). It is interesting that while in the neutral systems the inner C−S bonds iv are longer than the outer ones v, for the cations the opposite is true. The conformations of the SMe groups are noteworthy. In $\mathbf{15}^{2+}$, one SMe substituent at each dithiolium ring is coplanar with the ring and the other nearly perpendicular to it (torsion angles 9.4°, 2.1°, 82.7°, and 85.2°, respectively); bonds vii for the in-plane ligands are substantially shorter (and viii slightly shorter) than for the out-of-plane ones, indicating uneven conjugation. In $\mathbf{18}^{2+}$, all SMe groups adopt in-plane conformations, and bond distances are in agreement with those for similar groups in $\mathbf{15}^{2+}$. On the other hand, in the neutral systems there is no correlation between the Me−S−C=C torsion angles (varying from 178° to 102°) and the fairly constant C−S bond lengths.

Conclusions

The cyclophanes **18**−**20** have been synthesized by macrocyclization reactions of building blocks **15** and **16**, thereby providing a new structural modification of the 9,10-bis(1,3-dithiol-2-ylidene)-9,10-dihydroanthracene system. These are fundamentally interesting and unusual molecules by virtue of the combination of redox and structural properties which they display. This work paves the way for the synthesis of more elaborate caged and bridged structures on the basis of synthetic modifications and electrochemical manipulation of these versatile extended π-electron systems.

Experimental Section

General Procedures. All solvents were dried and distilled before use.

1-Chloro-2-{2-[(*tert*-butyldiphenylsilyl)oxy]ethoxy}-ethane (7). To a solution of 2-(2-chloroethoxy)ethanol **5** (9.97 g, 80.0 mmol) and imidazole (27.2 g, 400 mmol) in dry DMF (50 mL) was added *tert*-butyldiphenylchlorosilane (20.61 g, 75.0 mmol), and the reaction was stirred for 16 h at room temperature. The solution was poured onto water (500 mL) and extracted with hexane. The combined organic phases were washed with brine, dried ($MgSO_4$), and concentrated in vacuo to give a yellow oil. Purification by chromatography using a short column (silica gel, dichloromethane−hexane, 1:3 v/v) afforded **7** as a colorless oil (24.47 g, 90%). ^{1}H NMR ($CDCl_3$): δ 7.72−7.70 (4H, m), 7.44−7.40 (6H, m), 3.84 (2H, t, J = 5.6 Hz), 3.77 (2H, t, J = 6.0 Hz), 3.64 (2H, t, J = 5.6 Hz), 3.61 (2H, t, J = 6.0 Hz), 1.08 (9H, s). ^{13}C NMR ($CDCl_3$): δ 135.6, 133.5, 129.6, 127.6, 72.5, 71.4, 63.5, 42.8, 26.8, 19.2. MS (CI) m/z (%) 380 (67, MNH_4^+), 285 (100). Anal. Calcd for $C_{20}H_{27}ClO_2Si$ (MW 362.97): C, 66.18; H, 7.50. Found: C, 66.04; H, 7.45.

1-Iodo-2-{2-[(*tert*-butyldiphenylsilyl)oxy]ethoxy}-ethane (8). To a solution of 1-chloro-2-{2-[(*tert*-butyldiphenylsilyl)oxy]ethoxy}ethane **7** (24.30 g, 67 mmol) in dry 2-butanone (100 mL) was added sodium iodide (15.0 g, 100 mmol). The suspension was refluxed under argon for 48 h, concentrated in vacuo, and redissolved in dichloromethane (300 mL). The solution was washed with water and brine, dried ($MgSO_4$), and filtered through a plug of silica. Evaporation of the solvent in vacuo afforded **8** as a colorless oil (29.80 g, 98%). ^{1}H NMR ($CDCl_3$): δ 7.72−7.70 (4H, m), 7.44−7.38 (6H, m), 3.83 (2H, t, J = 5.0 Hz), 3.77 (2H, t, J = 6.5 Hz), 3.63 (2H, t, J = 5.0 Hz), 3.23 (2H, t, J = 6.5 Hz), 1.08 (9H, s). ^{13}C NMR ($CDCl_3$): δ 135.6, 133.5, 129.6, 127.6, 72.1, 72.0, 63.5, 26.8, 19.1, 3.1. MS (CI) m/z (%) 472 (48, MNH_4^+), 251 (100). Anal. Calcd for $C_{20}H_{27}IO_2Si$ (MW 454.42): C, 52.86; H, 5.99. Found: C, 52.95; H, 5.98.

2,6-Bis{2-[(*tert*-butyldiphenylsilyl)oxy]ethoxy}-anthraquinone (10). To a mixture of 1-bromo-2-[(*tert*-butyldiphenylsilyl)oxy]ethane **6** (prepared by direct analogy with **7** which is a modification of the literature route)[15] (16.35 g, 45.0 mmol) and potassium carbonate (4.15 g, 30.0 mmol) in dry degassed DMF (20 mL) was added anthraflavic acid **9** (3.60 g, 15.0 mmol). The reaction mixture was stirred under argon at 100 °C for 16 h, which made the color change from yellow to dark red, diluted with dichloromethane (300 mL), and washed with brine. The organic phase was dried ($MgSO_4$) and filtered through a plug of silica to give a yellow solution, which was concentrated in vacuo. The oily residue was purified by column chromatography (silica gel, dichloromethane−hexane, 1:1 v/v), and concentration in vacuo of the first yellow fraction afforded **10** as a pale yellow solid (9.18 g, 76%), mp 133−134 °C. ^{1}H NMR ($CDCl_3$): δ 8.23 (2H, d, J = 8.8 Hz), 7.80−7.78 (8H, m), 7.72 (2H, d, J = 2.4 Hz), 7.47−7.42 (12H, m), 7.19 (2H, dd, J_1 = 2.4 Hz, J_2 = 8.8 Hz), 4.29 (4H, t, J = 4.8 Hz),

(15) Paquette, L. A.; Doherty, A. M.; Rayner, C. M. *J. Am. Chem. Soc.* **1992**, *114*, 3910.

4.10 (4H, t, J = 4.8 Hz), 1.14 (18H, s). ^{13}C NMR ($CDCl_3$): δ 181.8, 163.6, 135.6, 135.5, 133.2, 129.7, 129.5, 127.6, 126.9, 120.7, 110.5, 69.6, 62.3, 26.7, 19.1. MS (CI) m/z (%) 805 (13, MH^+), 747 (20), 729 (100). Anal. Calcd for $C_{50}H_{52}O_6Si_2$ (MW 805.12): C, 74.59; H, 6.51. Found: C, 74.32; H, 6.56.

2,6-Bis{2-{2-[(*tert*-butyldiphenylsilyl)oxy]ethoxy}-ethoxy}anthraquinone (11). By a procedure similar to the synthesis of **10**, compound **11** was obtained from the reaction of anthraflavic acid **9** (3.60 g, 15.0 mmol) with 1-iodo-2-{2-[(*tert*-butyldiphenylsilyl)oxy]ethoxy}ethane **8** (16.35 g, 45.0 mmol) in the presence of potassium carbonate (4.15 g, 30.0 mmol). Purification by column chromatography (silica gel, dichloromethane) afforded **11** as a pale yellow solid (11.64 g, 87%), mp 103−104 °C. ^{1}H NMR ($CDCl_3$): δ 8.22 (2H, d, J = 8.8 Hz), 7.72 (2H, d, J = 2.8 Hz), 7.70−7.68 (8H, m), 7.42−7.34 (12H, m), 7.24 (2H, dd, J_1 = 2.8 Hz, J_2 = 8.8 Hz), 4.26 (4H, t, J = 4.6 Hz), 3.91 (4H, t, J = 4.6 Hz), 3.85 (4H, t, J = 5.2 Hz), 3.69 (4H, t, J = 5.2 Hz), 1.05 (18H, s). ^{13}C NMR ($CDCl_3$): δ 182.2, 163.7, 135.7, 135.6, 133.6, 129.6, 129.6, 127.6, 127.2, 121.2, 110.5, 72.7, 69.4, 68.2, 63.5, 26.8, 19.2. MS (CI) m/z (%) 910 (10, MNH_4^+), 815 (35). Anal. Calcd for $C_{54}H_{60}O_8Si_2$ (MW 893.22): C, 72.61; H, 6.77. Found: C, 72.52; H, 6.76.

2,6-Bis{2-[(*tert*-butyldiphenylsilyl)oxy]ethoxy}-9,10-bis[4,5-bis(methylthio)-1,3-dithiol-2-ylidene]-9,10-dihydroanthracene (13). To a solution of the phosphonate ester **12**[12] (1.72 g, 5.66 mmol) in dry tetrahydrofuran (100 mL) at −78 °C under argon was added lithium diisopropylamide (4.14 mL, 6.22 mmol of a 1.5 M solution) via syringe, and the resultant cloudy yellow mixture was stirred for 2 h at −78 °C. Compound **10** (1.90 g, 2.36 mmol) was dissolved in dry THF (30 mL) and added to the reaction mixture via a syringe over 15 min. The reaction mixture was stirred at −78 °C for another 2 h, whereupon it was allowed to slowly attain room temperature for 12 h. Evaporation of the solvent gave a red residue which was dissolved in dichloromethane (200 mL), washed with water and brine, dried ($MgSO_4$), and concentrated in vacuo. Column chromatography (silica gel, dichloromethane−hexane, 1:1 v/v) afforded **13** as a yellow foam (1.89 g, 69%), mp 82−85 °C. ^{1}H NMR ($CDCl_3$): δ 7.78−7.76 (8H, m), 7.48 (2H, d, J = 8.4 Hz), 7.46−7.40 (12H, m), 7.12 (2H, d, J = 2.8 Hz), 6.84 (2H, dd, J_1 = 2.8 Hz, J_2 = 8.4 Hz), 4.23−4.16 (4H, m), 4.07 (4H, t, J = 5.2 Hz), 2.41 (6H, s), 2.37 (6H, s), 1.12 (18H, s). ^{13}C NMR ($CDCl_3$): δ 157.1, 136.2, 135.6, 133.4, 129.6, 129.1, 127.7, 127.5, 126.5, 125.7, 125.5, 123.5, 111.9, 111.7, 69.2, 62.6, 26.8, 19.2, 19.0, 19.0. MS (CI): m/z = 1161 (13, MH^+), 283 (100). Anal. Calcd for $C_{60}H_{64}O_4S_8Si_2$ (MW 1161.85): C, 62.03; H, 5.55. Found: C, 61.65; H, 5.54.

2,6-Bis{2-{2-[(*tert*-butyldiphenylsilyl)oxy]ethoxy}-ethoxy}-9,10-bis[4,5-bis(methylthio)-1,3-dithiol-2-ylidene]-9,10-dihydroanthracene (14). This procedure is similar to the synthesis of **13**. The phosphonate ester **12**[12] (4.00 g, 13.1 mmol) was deprotonated using lithium diisopropylamide (9.60 mL, 14.4 mmol of a 1.5 M solution) and reacted with compound **11** (4.70 g, 5.26 mmol). Purification by column chromatography (silica gel, dichloromethane−hexane, 3:1 v/v) afforded **14** as a yellow foam (5.33 g, 81%), mp 51−54 °C. ^{1}H NMR ($CDCl_3$): δ = 7.71−7.68 (8H, m), 7.43 (2H, d, J = 8.8 Hz), 7.41−7.34 (12H, m), 7.07 (2H, d, J = 2.4 Hz), 6.83 (2H, dd, J_1 = 2.4 Hz, J_2 = 8.8 Hz), 4.15 (4H, t, J = 4.8 Hz), 3.89−3.84 (8H, m), 3.69 (4H, t, J = 5.2 Hz), 2.38 (6H, s), 2.34 (6H, s), 1.06 (18H, s). ^{13}C NMR ($CDCl_3$): δ 157.1, 136.2, 135.6, 133.6, 129.6, 129.2, 127.7, 127.6, 126.6, 126.1, 125.4, 123.5, 112.2, 111.5, 72.7, 69.7, 67.7, 63.5, 26.8, 19.2, 19.2, 19.1. MS (CI): m/z = 1249 (14, MH^+), 283 (100). Anal. Calcd for $C_{64}H_{72}O_6S_8Si_2$ (MW 1249.95): C, 61.50; H, 5.81. Found: C, 61.23; H, 5.84.

2,6-Bis(2-hydroxyethoxy)-9,10-bis[4,5-bis(methylthio)-1,3-dithiol-2-ylidene]-9,10-dihydroanthracene (15). Compound **13** (1.70 g, 1.47 mmol) was dissolved in dry THF (20 mL) and stirred under argon at room temperature. A solution of tetrabutylammonium fluoride (4.40 mL, 4.40 mmol of a 1.0 M solution in THF) was added dropwise via a syringe over 15 min, causing the reaction mixture to change color from yellow to brown. Further stirring for 1.5 h, followed by addition of a few drops of water (0.1 mL) and evaporation of the solvent, afforded a brown residue. The residue was dissolved in dichloromethane (200 mL), washed with water and brine, dried ($MgSO_4$), and concentrated in vacuo. Chromatography using a short column (silica gel, dichloromethane until no more byproducts were visible on the column, then dichloromethane-ethyl acetate, 3:1 v/v) afforded **15** as a yellow solid (0.938 g, 93%), mp 147−150 °C. Yellow-brown prisms, suitable for X-ray crystallographic analysis, were grown by slow diffusion of hexane into a solution of **15** in dichloromethane. ^{1}H NMR ($CDCl_3$): δ 7.44 (2H, d, J = 8.8 Hz), 7.08 (2H, d, J = 2.4 Hz), 6.84 (2H, dd, J_1 = 2.4 Hz, J_2 = 8.8 Hz), 4.15 (4H, t, J = 4.8 Hz), 4.01 (4H, t, J = 4.8 Hz), 2.39 (12H, s), 1.94 (2H, br s). ^{13}C NMR ($CDCl_3$): δ 156.9, 136.3, 129.6, 128.0, 126.7, 126.3, 125.3, 123.2, 112.0, 111.6, 69.4, 61.4, 19.2, 19.1. UV−vis (CH_2Cl_2): λ_{max} (lg e) 432 (4.40), 364 (4.18) nm. MS (EI) m/z (%) 684 (100, M^+). Anal. Calcd for $C_{28}H_{28}O_4S_8$ (MW 685.05): C, 49.09; H, 4.12. Found: C, 49.10; H, 4.20.

2,6-Bis[2-(2-hydroxyethoxy)ethoxy]-9,10-bis[4,5-bis-(methylthio)-1,3-dithiol-2-ylidene]-9,10-dihydroanthracene (16). By a procedure similar to that for the conversion of **13** to **15**, compound **14** (5.00 g, 4.00 mmol) was treated with tetrabutylammonium fluoride (12.0 mL, 12.0 mmol of a 1.0 M solution in THF) to form **16**. Purification by chromatography using a short column (silica gel, dichloromethane until no more byproducts were visible on the column, then ethyl acetate) afforded **16** as a yellow solid (2.68 g, 87%), mp 204−205 °C. ^{1}H NMR ($CDCl_3$): δ 7.43 (2H, d, J = 8.8 Hz), 7.07 (2H, d, J = 2.8 Hz), 6.84 (2H, dd, J_1 = 2.4 Hz, J_2 = 8.4 Hz), 4.20 (4H, t, J = 4.8 Hz), 3.90 (4H, t, J = 4.8 Hz), 3.78 (4H, t, J = 4.8 Hz), 3.69 (4H, t, J = 4.8 Hz), 2.38 (12H, s), 1.98 (2H, br s). ^{13}C NMR ($CDCl_3$): δ 156.9, 136.3, 129.4, 127.8, 126.6, 126.3, 125.3, 123.3, 112.2, 111.6, 72.6, 69.6, 67.6, 61.8, 19.2, 19.1. UV−vis (CH_2Cl_2): λ_{max} (log ϵ) 432 (4.41), 364 (4.18) nm. MS (EI) m/z (%) 772 (100, M^+). Anal. Calcd for $C_{32}H_{36}O_6S_8$ (MW 773.15): C, 49.71; H, 4.69. Found: C, 49.77; H, 4.73.

Cyclophane (18) and Cyclophane (20). To a solution of dialcohol **15** (0.300 g, 0.438 mmol) and 1,4-benzenedicarbonyl chloride **17** (0.089 g, 0.438 mmol) in dry dichloromethane (300 mL) was added triethylamine (0.50 mL, excess), and the reaction was stirred under argon for 16 h at room temperature. The solution was concentrated in vacuo and the orange residue purified by column chromatography (silica gel, dichloromethane). The fractions containing the first yellow band were concentrated in vacuo to give **18** as a yellow powder (0.141 g, 39%). Orange-yellow prisms, suitable for X-ray crystallographic analysis, were grown by slow diffusion of hexane into a solution of **18** in dichloromethane, mp >260 °C. ^{1}H NMR ($CDCl_3$): δ 7.38 (2H, d, J = 8.4 Hz), 7.36 (2H, d, J = 2.4 Hz), 6.95 (2H, dd, J_1 = 2.4 Hz, J_2 = 8.4 Hz), 6.89 (4H, s), 4.67−4.55 (6H, m), 4.47−4.41 (2H, m), 2.39 (6H, s), 2.38 (6H, s). ^{13}C NMR ($CDCl_3$): δ 165.0, 158.3, 136.6, 132.9, 130.1, 128.8, 128.7, 126.6, 125.9, 125.6, 122.5, 115.3, 114.2, 67.0, 66.2, 19.1, 19.0. UV−vis (CH_2Cl_2): λ_{max} (log ϵ) 436 (4.55), 368 (4.36) nm. MS (EI) m/z (%) 814 (100, M^+). Anal. Calcd for $C_{36}H_{30}O_6S_8$ (MW 815.15): C, 53.04; H, 3.71. Found: C, 52.81; H, 3.68.

The second yellow broad band was collected, concentrated in vacuo, and recolumned (silica gel, dichloromethane−ethyl acetate 98:2 v/v), affording **20** as a yellow powder (0.083 g, 23%), mp 222−227 °C (dec). Orange prisms, suitable for X-ray crystallographic analysis, were grown by slow diffusion of hexane into a solution of **20** in dichloromethane. ^{1}H NMR ($CDCl_3$): δ 7.98 (4H, s), 7.94 (4H, s), 7.412 (2H, d, J = 8.4 Hz), 7.408 (2H, d, J = 8.8 Hz), 7.10 (4H, d, J = 2.4 Hz), 6.87 (2H, dd, J_1 = 2.8 Hz, J_2 = 8.4 Hz), 6.85 (2H, dd, J_1 = 2.8 Hz, J_2 = 8.4 Hz), 4.76−4.68 (8H, br m), 4.42−4.38 (8H, br m), 2.34−2.33 (24H, m). UV−vis (CH_2Cl_2): λ_{max} (log ϵ) 432 (4.73), 368 (4.53) nm. MS (EI) m/z (%) 1628 (1, M^+), 1627 (2), 182 (100). Anal. Calcd for $C_{72}H_{60}O_{12}S_{16}$ (MW 1630.30): C, 53.04; H, 3.71. Found: C, 52.77; H, 3.67.

Cyclophane (19). By a procedure similar to that for the conversion of **15** to **18**, dialcohol **16** (0.250 g, 0.320 mmol) was reacted with 1,4-benzenedicarbonyl chloride **17** (0.066 g, 0.320 mmol) in the presence of excess triethylamine. Purification by column chromatography (silica gel, dichloromethane−ethyl acetate, 95:5 v/v) afforded **19** as a yellow powder (0.083 g, 28%). Yellow prisms, suitable for X-ray crystallographic analysis,

were grown by slow diffusion of hexane into a solution of **19** in dichloromethane, mp 209−211 °C. ^{1}H NMR ($CDCl_3$): δ 7.35 (4H, s), 7.26 (2H, d, J = 3.2 Hz), 7.20 (2H, d, J = 8.4 Hz), 6.70 (2H, dd, J_1 = 2.4 Hz, J_2 = 8.4 Hz), 4.58−4.54 (2H, m), 4.41−4.37 (2H, m), 4.31−4.28 (4H, m), 4.06−4.02 (2H, m), 3.92−3.83 (6H, m), 2.373 (6H, s), 2.367 (6H, s). ^{13}C NMR ($CDCl_3$): δ 165.6, 157.3, 136.0, 133.0, 129.0, 128.9, 127.5, 126.3, 126.2, 125.3, 123.6, 113.2, 111.9, 70.1, 69.6, 69.2, 64.8, 19.2, 19.0. UV−vis (CH_2Cl_2): λ_{max} (log ϵ) 432 (4.58), 364 (4.37) nm. MS (EI) m/z (%) 902 (100, M^+). Anal. Calcd for $C_{40}H_{38}O_8S_8$ (MW 903.25): C, 53.19; H, 4.24. Found: C, 52.87; H, 4.21.

Preparation of $15^{2+}(ClO_4^-)_2$. Dry tetrabutylammonium perchlorate (50 mg) was added to each chamber of a glass electrocrystallization cell, in which the two chambers were separated by a glass frit, and the cell was flushed with argon. Compound **15** (5 mg) was placed in the anodic chamber, and dry degassed dichloromethane (7 mL) was added to each chamber of the cell. The platinum electrodes were mounted, sealing the solutions from the atmosphere. A potential of 1.0 V was applied, which provided an initial current of 1.0 μA. The cell was stored in the dark for 14 days at 20 °C, during which time the current dropped to 0.2 μA and red needles of $\mathbf{15}^{2+}(ClO_4^-)_2$ (up to 5 mm in length) grew on the anode. The crystals, which were suitable for X-ray crystallography, were harvested and washed with dry dichloromethane.

Preparation of $18^{2+}(I_3^-)_2(I_2)_{0.5}CH_2Cl_2$. A 10 mM solution of cyclophane **18** (2 mL) in dichloromethane was placed in a 5 mL open sample vial which was placed in a sealed 250 mL sample vial containing iodine crystals (0.5 g). Diffusion of iodine vapor into the solution of **18** gave black shiny needles suitable for X-ray crystallographic analysis, mp 195−197 °C (dec). Anal. Calcd for $C_{36}H_{30}O_6S_8(I_3)_2(I_2)_{0.5}CH_2Cl_2$: C, 24.85; H, 1.80. Found: C, 24.95; H, 1.75.

Crystal Structure Analyses. X-ray diffraction experiments were carried out on a SMART 3-circle diffractometer with a 1K CCD area detector, using graphite-monochromated Mo Kα radiation ($\bar{\lambda}$ = 0.71073 Å) and a Cryostream (Oxford Cryosystems) open-flow N_2 gas cryostat. For **18** and **19**, the full sphere of the reciprocal space was covered by a combination of five sets of ω scans; each set at different φ and/or 2θ angles; for the rest, more than hemisphere was covered by four sets. Reflection intensities were integrated using SAINT program[16] and corrected for absorption by numerical integration methods (based on crystal face indexing) for **18**, **19**, $\mathbf{18}^{2+}$, and $\mathbf{15}^{2+}$ or by semiempirical method (comparison of Laue equivalents)[17] for **15**. The structures were solved by direct methods and refined by full-matrix least squares against F^2 of all data, using SHELXTL software.[18] Crystal data and experimental details are summarized in Table 4 (Supporting Information), and atomic coordinates, thermal parameters, and bond distances and angles have been deposited at the Cambridge Crystallographic Data Centre.[19]

Acknowledgment. We thank EPSRC and the Danish Research Academy (C.A.C.) for funding. J.A.K.H. thanks the EPSRC for a Senior Research Fellowship.

Supporting Information Available: ^{1}H NMR spectra of compounds **7**, **8**, **10**, **11**, **13**, **14**, **15**, **16**, **18**, **19**, and **20** and the crystallographic data for **15**, $\mathbf{15}^{2+}(ClO_4^-)_2$, **18**, $\mathbf{18}^{2+}(I_3^-)_2\cdot(I_2)_{0.5}$, **19**, and **20**. This material is available free of charge via the Internet at http://pubs.acs.org.

JO001524K

(16) *SMART* & *SAINT*, Area detector control & integration software, Ver. 6.01. Bruker Analytical X-ray Systems, Madison, WI, 1999.

(17) Sheldrick, G. M. *SADABS:* Program for scaling and correction of area detector data. University of Göttingen, Germany, 1996.

(18) *SHELXTL*, An integrated system for solving, refining and displaying crystal structures from diffraction data, Ver. 5.10. Bruker Analytical X-ray Systems, Madison, WI, 1997.

(19) Supplementary publication nos. CCDC-137171, 149466, 137172, 149465, 149467, and 149468 for **15**, $\mathbf{15}^{2+}$, **18**, $\mathbf{18}^{2+}$, **19**, and **20**, respectively, can be obtained on request from the Director, Cambridge Crystallographic Data Centre, 12 Union Road, Cambridge, CB2 1EZ, U.K.